Biomedicine & Pharmacotherapy 161 (2023) 114536

Contents lists available at ScienceDirect

Biomedicine & Pharmacotherapy

journal homepage: www.elsevier.com/locate/biopha

High potency of magnetic iron oxide nanoparticles covered by piroctone olamine against cystic echinococcosis

Yosra Raziani [a], Koroush Cheraghipour [b], Mojtaba Shakibaie [c], Javad Ghasemian Yadegari [b], Hossein Mahmoudvand [b,*]

[a] Nursing Department, Al-Mustaqbal University College, 51001 Hillah, Babylon, Iraq
[b] Razi Herbal Medicines Research Center, Lorestan University of Medical Sciences, Khorramabad, Iran
[c] Pharmaceutics Research Center, Institute of Neuropharmacology, Kerman University of Medical Sciences, Kerman, Iran

ARTICLE INFO

Keywords:
Nanomedicine
Protoscolicidal
Hydatid cyst
Apoptosis
Scolicidal

ABSTRACT

This study examined the synthesis of magnetic iron oxide nanoparticles coated with PO (FOMNPsP) and assessed their in vitro, *ex vivo,* and in vivo effects against cystic echinococcosis. The FOMNPsP was synthesized through the alkalization of iron ions in a deoxygenated form. *In vitro* and *ex vivo* protoscolicidal effects of FOMNPsP (100–400 μg/mL) were evaluated on hydatid cyst protoscoleces by the eosin exclusion test for 10–60 min. The effect of FOMNPsP on caspase-3 gene expression and exterior ultra-structural of protoscoleces was assessed by real-time PCR and scanning electron microscopy (SEM), respectively. *In vivo* effects were assessed by evaluating the number, size, and weight of hydatid cysts among infected mice. The FOMNPsP size was < 55 nm, and the most frequent particles were in the 15–20 nm range. *In vitro* and *ex vivo* assays revealed that the highest protoscolicidal effect was observed at 400 μg/mL with 100% lethality. After exposure of protoscoleces with FOMNPsP, the level of gene expression of caspase-3 was dose-dependently increased ($p < 0.05$). By SEM, the FOMNPsP-treated protoscoleces showed wrinkles and bulges resulting from the formation of blebs. FOMNPsP significantly decreased ($p < 0.01$) the mean number, size, and weight of the hydatid cyst. FOMNPsP revealed the potent protoscolicidal traits through disrupting the cell wall and apoptosis induction. The results also indicated the promising effect of FOMNPsP in controlling hydatid cysts in the animal model. Although FOMNPsP is safe for human normal cells, more investigations are required to clarify its toxicity and precise mechanisms of action.

1. Introduction

Cystic echinococcosis (CE) or hydatid cyst disease is one of the most prevalent infections among humans and animals, triggered by the larval form of the *Echinococcus granulosus* cestode. Larval infection (hydatid disease) is linked to the continuing development of cysts in the intermediate host [1]. Humans, as accidental hosts, become infected by ingesting parasite eggs (excreted from dogs), along with the consumption of vegetables and fruits, drinking water, and having contact with infected dogs [2]. After an indeterminate period of several months to years, the disease may become symptomatic as widespread lesions, although 60% of infections are asymptomatic [3]. Cysts usually appear in the liver (47–78%) and lungs (8–35%) and rarely affect other organs such as the spleen, brain, kidneys, peritoneal cavity, muscles, bones, and heart (4–24%) [4,5].

The typical approach to CE is surgery, but in patients with numerous cysts in critical organs or in high-risk patients, pharmacotherapy with albendazole, mebendazole, amphotericin B, praziquantel, etc. is administered [6]. Although the risk of protoscoleces' leakage increases during surgery, which is the most common cause of disease recurrence, however, the use of protoscolicidal agents can reduce the recurrence rate [7]. Among the most important protoscolicidals, 0.5% silver nitrate ($AgNO_3$), 10% or 20% hypertonic saline, and hydrogen peroxide are the most common agents [8]. Nevertheless, recent studies have reported that these chemical agents have side effects such as liver fibrosis [8–10].

Magnetic nanoparticles are biological resources with a wide range of biological and therapeutic properties [11]. Among these nanoparticles, magnetic iron oxide nanoparticles (FOMNPs) are broadly applied as a proper antimicrobial delivery system to infected sites due to their high site-specific delivery power [12]. FOMNPs also display potent antimicrobial effects against some microbial pathogens, e.g., *Candida* spp., *Enterococcus spp*, *Escherichia coli*, and *Leishmania spp.*, [13].

* Corresponding author.
E-mail addresses: dmahmodvand@gmail.com, mahmoudvand.h@lums.ac.ir (H. Mahmoudvand).

https://doi.org/10.1016/j.biopha.2023.114536
Received 3 February 2023; Received in revised form 9 March 2023; Accepted 13 March 2023
Available online 20 March 2023

Pyroctoneolamine (PO) (1-hydroxy-4-methyl-6-(2,4,4-trimethylpentyl)-2(1H)-pyridone) is a pyridone derivate with strong bactericidal and fungicidal effects [14]. PO is reported to exhibit antimicrobial effects by disrupting microbes' cell membranes and stopping metabolism energy and oxygen uptake [15].

The efficacy of various synthesized nanoparticles against CE has been reported in recent years; however, reliable findings have not been reported due to some limitations in studies, e.g., differences in results, unclear cytotoxicity, lack of a study on animal models (in vivo), and the non-specified mechanisms of action of the tested nanoparticles [16]. Given the biological and pharmacological effects of iron oxide nanoparticles, the current study examined the synthesis of magnetic iron oxide nanoparticles coated with PO (FOMNPsP) and thoroughly investigated the in vitro and *ex vivo* effects of the protoscolicidal, mechanisms of action (e.g., apoptosis induction and affecting the structure of the parasite), cytotoxicity, and their effect on the hydatid cyst in an animal model.

2. Materials and methods

2.1. FOMNPsP synthesis

The FOMNPsP was synthesized through the alkalization of Fe2 + and Fe3 + ions (≥99.9% purity, Merck, Germany) in a deoxygenated form based on a previously described method [17]. FOMNPsP was prepared according to the precipitation process by coating FOMNPs with PO [17]. To this end, Fe3O4 NPs (100 mg) were dissolved in deionized water (100 mL) by ultrasonication (100 W) for 10 min. Next, 2 mL of the PO solution (30 mg/mL, Sigma–Aldrich, USA) was gradually added to the mixture with continuous stirring (300 rpm) by a magnetic stirrer (Joan Lab Equipment (Zhejiang) Co., Ltd. China). Subsequently, the attained solution was kept at 45 °C for 20 min, and then, the PO-coated Fe3O4 NPs were separated from the mixture by using a magnet. After the NPs were washed with deionized water, they were lyophilized and kept at 4 °C until testing.

2.2. Characterization of the NPs

Transmission electron microscopy (TEM, Zeiss 902 A, Germany) was used to characterize the NPs. Zetasizer MS2000 (Malvern, Worcestershire, WR14 1XZ. UK) and a P3000 diffractometer tool (Rich Seifert, NY, USA) were applied to obtain the particle size and information of X-ray diffraction (XRD). Fourier-transform infrared (FTIR) spectroscopy using a PerkinElmer (Wellesley, MA, 02481, USA) and UV-Vis spectroscopy analysis by a UV–visible spectrophotometer (UVD-2950; Labomed, USA) were also applied to study the crystalline nanoparticles and identify the functional groups and biomolecules responsible for the synthesis and coverage of nanoparticles, respectively.

2.3. Protoscoleces preparation

This study was conducted experimentally on *E. granulosus* protoscoleces prepared from liver cysts of infected sheep from a slaughterhouse in Khorramabad, Iran. Infected livers containing hydatid cysts were transferred to the parasitology laboratory under sterile conditions. Then, the required protoscoleces were removed from the cysts, moved to sterile tubes, and washed with sterile normal saline at least three times [18].

2.4. Viability test

After obtaining the protoscoleces, their viability was checked by the movement of flame cells and 0.1% eosin staining (≥95% purity, Sigma-Aldrich, Germany) [19]. By counting 100 protoscoleces, only cysts whose viability was above 90% were used for further testing. In this test, viable protoscoleces remained colorless, while dead ones turned pink

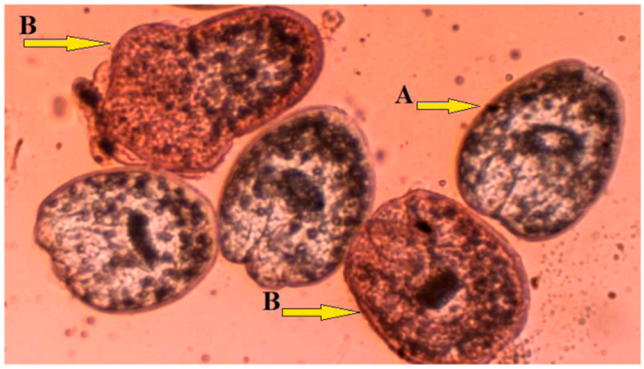

Fig. 1. The viable colorless protoscoleces (A) and dead pink protoscoleces (B) after exposure with tested drugs.

(Fig. 1).

2.5. In vitro protoscolicidal effects

To study the in vitro protoscolicidal effect of FOMNPsP, first, 100–400 μg/mL of nanoparticles (the selection of these concentrations was based on preliminary tests) was separately mixed with a suspension of protoscoleces (1 $\times 10^3$/mL) and left for 10, 20, 30, and 60 min. By adding 50 μL of 0.1% eosin stain to the treated parasites, the smears were prepared on a glass slide and covered with a coverslip, and the viability of the tested parasites was examined under a light microscope. Normal saline and $AgNO_3$ (10%, Sigma-Aldrich, Germany) were the negative and positive control, respectively [20].

2.6. Ex vivo protoscolicidal effects

For each concentration of FOMNPsP (100–400 μg/mL), three hydatid cysts were used. First, half of the content of the cyst was emptied, and then, different concentrations of nanoparticles were injected into the cyst to fill the whole cyst. Next, a low volume of the cyst fluid was obtained in 5, 10, 15, 20, 30, and 60 min, and viability was measured similarly to the in vitro method [21].

2.7. Evaluation of caspase-3 activity of iron nanoparticles on protoscoleces

After treating and exposing the protoscoleces to different concentrations of FOMNPsP, an RNA commercial kit (CinnaGen, Tehran, Iran) was employed for RNA extraction. Complementary DNA (cDNA, CinnaGen, Tehran, Iran) was synthesized using 1 μg of total RNA, random hexamer primer. The thermal condition was an initial denaturation step at 96 °C for 4 min and, then, 35 cycles at 95 °C for 30 s, followed by 58 °C for 40 s, and 73 °C for 40 s. PCR amplification was also performed in triplicate. Finally, $\Delta\Delta Ct^{-2}$ was calculated using the optical system software (iQTM5, Bio-Rad, Hercules, CA, USA) and β-actin was applied to normalize the mRNA levels of the tested samples [22]. The sequence of the used primers was as follows:

Caspase-3F: 5′-TTCATTATTCAGGCCTGCCGAGG-3′.
Caspase-3R: 5′-TTCTGACAGGCCATGTCATCCTCA-3.
β-actinF: GTGACGTTGACATCCGTAAAGA.
β-actin R: GCCGGACTCATCGTACTCC.

2.8. Exterior ultra-structural effects of NPs on protoscoleces

Initially, the protoscoleces were fixed in glutaraldehyde (2.5%) at 21 °C for 4 h. After the protoscoleces were washed with phosphate-buffered saline (PBS), the dehydration procedure was started in alcohol ascending grades (50–100% V/V) for 15 min. Next, the protoscoleces reached the last level of drying via a dryer apparatus (S4160,

Hitachi, Japan) for 40 min. Then, the treated protoscoleces were on a metal stub and sputter-coated in gold using a SEM covering tool (E5100 Polaron, Milton Keynes, UK). The covered specimens were then assessed via scanning electron microscopy (SEM, 6400 JEOL, Ltd., Tokyo, Japan) at an acceleration voltage of 15–25 KV.

2.9. Cytotoxicity effects of FOMNPsP

Human normal embryonic kidney (HEK293) and human hepatocellular carcinoma (HepG2) cell lines procured from Pasteur Institute (Tehran, Iran) were cultured in Dulbecco's Modified Eagle Medium (DMEM, Merck, Germany) improved with Pen-Strep (100 μg/mL, Merck, Germany) and 10% fetal bovine serum (FBS, Merck, Germany) at 37 °C in 5% CO_2. To determine the cytotoxic effects, 0.1 mL of the cells (1×10^5/mL) exposed to various concentrations of FOMNPsP was placed in the wells and incubated at 24 °C for 48 h. After MTT solution (5 mg/mL, Sigma-Aldrich, Darmstadt, Germany) was added to the wells, the plate was incubated for 4 h. Then, DMSO was added to the wells and, after 30 min, the absorption of the wells was read by an ELISA reader (ELISA Plate Reader, BioTek 800 TS – Agilent, USA) at the absorption wavelength of 570 nm. The cytotoxic concentrations of 50% (CC_{50}) were obtained via Probit examination in IBM SPSS Statistics for Windows 26.0 (IBM Corp., Armonk, N.Y., USA). [23]. Finally, the selective index (SI= CC_{50} of healthy cells / CC_{50} of cancer cells) expressed the selective toxicity of the Fe3O4 NPs against cancer cells and healthy cells.

2.10. In vivo effect of NPs on hydatid cysts in mice

2.10.1. Animals

Forty 40–60-day-old male BALB/c mice (25–30 g) were prepared from the Animal House of Lorestan University of Medical Sciences (Khorramabad, Iran). The animals were kept under normal situations with a 12:12 h dark/light cycle with access to food and water.

2.10.2. Establishment of hydatid cysts in mice

The mice were randomly allocated to four groups of 10 mice each. Then, they were all infected intraperitoneally with 0.5 mL of sterile PBS containing 2×10^3 viable protoscoleces [24]. Twelve weeks post-infection, one mouse from each group was randomly selected and deeply anesthetized with ether, and the hydatid cysts were observed in the peritoneal cavity.

2.10.3. Treatment of mice with hydatid cysts

The infected mice orally received (i) albendazole at 200 mg/kg/day for 28 days; (ii) FOMNPsP at 20 mg/kg/day for 28 days; (iii) FOMNPsP at 40 mg/kg/day for 28 days; (iv) normal saline for 28 days. After 28 days, the mice were euthanized; after the peritoneal cavity was opened, the internal organs were checked for hydatid cysts and cautiously collected. *In vivo* effects of FOMNPsP were assessed by calculating the number, size, and weight of hydatid cysts among the tested groups.

2.11. Data analysis

All in vitro and *ex vivo* experiments were repeated in triplicate. After data collection, descriptive statistics were used to describe the data by calculating the central tendency and dispersion indices. To compare the groups, one-way analysis of variance (ANOVA) and repeated measure ANOVA were used. All statistical tests were performed in IBM SPSS Statistics for Windows 26.0 (IBM Corp., Armonk, N.Y., USA), and $p < 0.05$ was considered significant.

3. Results and discussion

The characterization of the synthesized FOMNPsP is fully reported in Supplementary File 1. Checking the XRD pattern of FOMNPsP with characteristic peaks ranging from 30.1∘ to 74∘ confirmed the correct synthesis of NPs; however, the PO covering process had no obvious effect on the crystalline construction of NPS. In line with our results, Gan et al. (2011) confirmed that covering FOMNPs via boronic acid does not significantly alter the XRD pattern of NPs [24]. The findings showed that FOMNPsP and FOMNPs exhibited saturation magnetization (MS) values of < 45 and 90 emu/g, respectively. This difference in MS values of NPs is likely linked to the larger size of FOMNPs and the appearance of PO on the NPs' surface. Wei et al. (2012) reported that the variation of Fe3O4 surface via oleic acid and sodium citrate exhibited reduced MS in NPs [25,26].

Functional groups located on the NP's surface were identified by the FTIR analysis. The considerable absorption of the Fe–O bond at 632 cm^{-1} was observed in FOMNPs. The predominant peaks at 627, 1190, 1366, 1500, 1625, and 3000 cm^{-1} were linked to Fe–O, C-O, C-N, C═C, C═O, N-H, and O-H groups, respectively. In addition, the analogous peaks in the FTIR PO spectrum represented that the covering procedure was properly performed. TEM was applied to estimate the size and shape of NPs before and after the covering process. The size of the FOMNPsP and FOMNPs was < 55 nm and < 40 nm, respectively, while the most frequent particles in FOMNPs and FOMNPsP exhibited the size of 10–15 and 15–20 nm, respectively. Aggregation of the synthesized NPs is probably due to the wide surface of the NPs and the magnetic powers surrounded by NPs [27]. The covering of NPs with PO increased the NP size. Similarly, Khorramizadeh et al. (2010) found that covering magnetic NPs with umbelliprenin increased the NP size [17].

The in vitro protoscolicidal activities of the synthesized NPs are depicted in Fig. 2. With raising the concentration, the protoscolicidal effect of NPs increased in a dose-dependent manner ($p < 0.001$). Among the concentrations of FOMNPsP, the highest protoscolicidal effect belonged to the concentration of 400 μg/mL with 100% lethality after 10 min of exposure to hydatid cyst protoscoleces. As for other concentrations, the rate of the highest anti-parasitic effect for concentrations of 300, 200, and 100 μg/mL was 100% (after 20 min), 100% (after 30 min), and 73.2% (after 60 min), respectively. The lethality rate of protoscoleces in normal saline and $AgNO_3$ was 4.23% and 100% after 60 and 5 min of exposure, respectively.

Although the NPs showed a significant protoscolicidal effect in *ex vivo* similar to in vitro conditions, the concentrations tested *ex vivo* required more incubation time for the effectiveness and protoscolicidal effect of NPs (Fig. 3). FOMNPsP at concentrations of 400 and 300 μg/mL displayed their protoscolicidal effects with 100% lethality after 20 and 30 min of treatment, respectively. Additionally, NPs at concentrations of 200 and 100 μg/mL exhibited their protoscolicidal effect as 79.6% and 42.7% after 60 min of exposure, respectively.

As shown in Fig. 4, the real-time PCR showed that after exposure of protoscoleces to FOMNPsP, the gene expression level of caspase-3 dose-dependently increased compared with the control group ($p < 0.05$). The SEM results demonstrated that in the control group (protoscoleces treated with normal saline), the smoothness and integrity of the protoscoleces were observed, while in the treatment group (protoscoleces treated with FOMNPsP at 400 μg/mL), wrinkles and bulges appeared due to the formation of blebs (Fig. 5). Considering the cytotoxicity effects of FOMNPsP, the results of the cell viability assay showed that the CC_{50} value of FOMNPsP for HepG2 and HEK293 was 246.1 and 537.4 μg/mL, respectively. The SI was 2.18 (>2), indicating that FOMNPsP is safe for healthy cells (Fig. 6).

By in vivo assay, the macroscopic examinations showed that all the hydatid cysts were hepatic and peritoneum cysts. The highest size, the largest number, and the greatest weight of hydatid cysts belonged to the mice of the negative control group that received normal saline for 28 days (Fig. 7). As shown in Table 1, after treatment of mice with FOMNPsP, especially at the dose of 40 mg/mL, the mean number, size, and weight of the hydatid cyst significantly decreased ($p < 0.01$). In addition, albendazole at 200 mg/kg significantly declined the mean number, size, and weight of hydatid cysts in comparison with the control group.

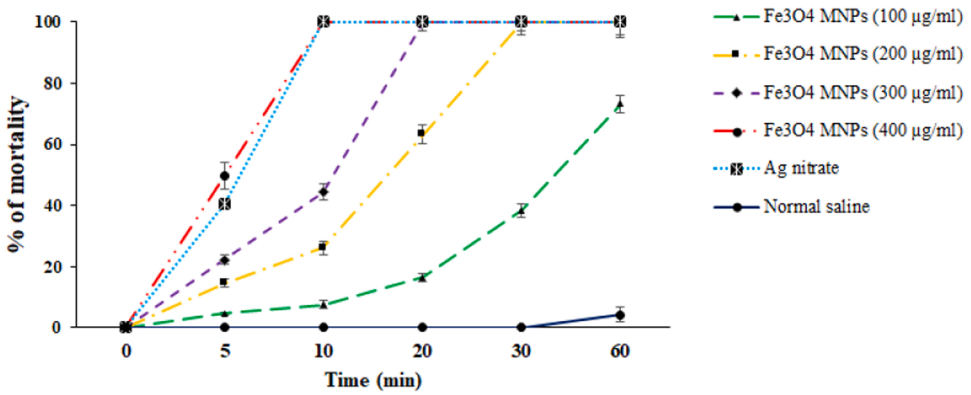

Fig. 2. In vitro effects of the various concentrations magnetic iron oxide nanoparticles covered by piroctone olamine on the mortality rate hydatid cyst protoscoleces in different time. Mean±SD (n = 3).

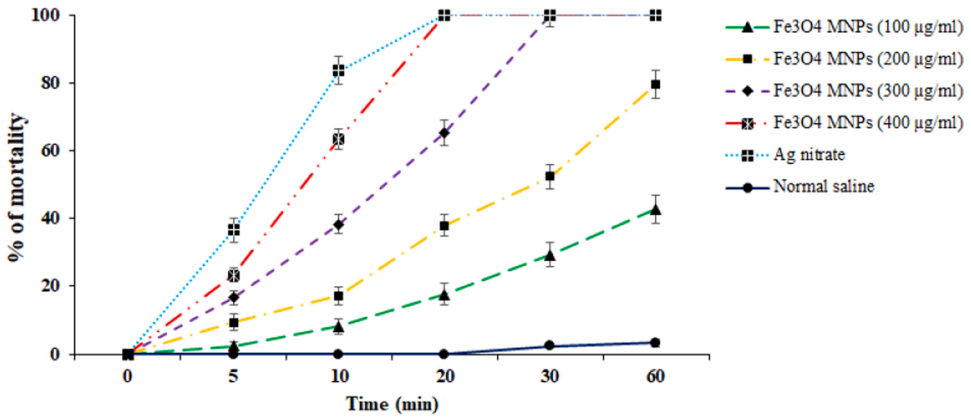

Fig. 3. Ex vivo effects of the various concentrations magnetic iron oxide nanoparticles covered by piroctone olamine on the mortality rate hydatid cyst protoscoleces in different time. Mean±SD (n = 3).

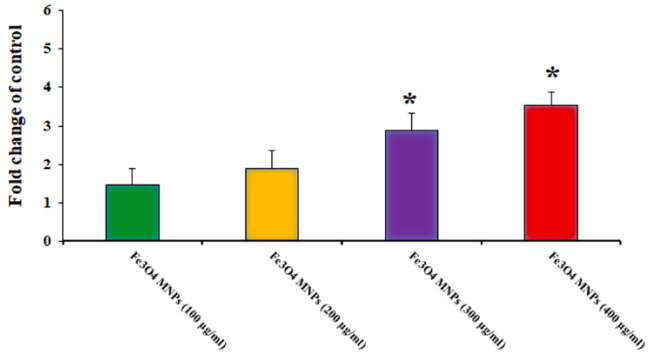

Fig. 4. Effect of different concentrations of magnetic iron oxide nanoparticles covered by piroctone olamine on the level of gene expression of Caspase-3 in hydatid cyst protoscoleces. Mean ± SD (n = 3). *$P < 0.001$.

Concerning the anti-parasitic effects of iron magnetic nanoparticles, Khatami et al. (2017) found that iron oxide nanoparticles were effective on the growth rate of the promastigotes of *L. major* with the IC_{50} value of 350 µg/mL [28]. Dorostkar et al. (2017) also reported that iron oxide nanoparticles at the doses of 0.004–0.012% w/v predominantly elevated the lethality rate of *Toxocara vitulorum* [29]. Moreover, Kannan et al. (2019) found that FeONPs significantly strengthened the effect of artesunate against andartemisinin-resistant *Plasmodium falciparum* in human blood and mice infected with *P. berghei* ANKA [30].

In recent years, resistance to antiparasitic agents mainly through genetic changes has made parasitic infections rigid to treatment and increased the risk of infection spread, severe illness, and death [31]. It has been proven that nanoparticles can overcome drug-resistance mechanisms due to their unique physio-chemical possessions, enabling multiple new antiparasitic pathways to complete antimicrobial activity [32]. Concerning the antimicrobial mechanisms of iron oxide nanoparticles, although the accurate mechanisms of action are not still understood, previous studies showed that these particles display their antimicrobial mechanisms by disturbing the outer and inner cell wall membranes, increasing reactive oxygen species (ROS), arresting the cell enzymatic activity, disrupting proteins and DNA, and inducing apoptosis [33, 34].

The strength of this study lies in the full examination of pre-clinical tests (e.g., in vitro, *ex vivo,* and in vivo) against protoscoleces and hydatid cysts, examination of the cytotoxicity of synthetic nanoparticles, and studying some possible anti-parasitic mechanisms of these nanoparticles. On the other hand, not investigating the mechanisms of the action and possible toxicity of FOMNPsP in hydatid cyst control in the animal model is the main weakness of the present study. We hope that by clarifying all aspects of the effectiveness, mechanisms of action, and toxicity of these nanoparticles, especially in human cases, they can be introduced as a new agent in the treatment of hydatid cysts. However, the reduction of circulation half-time and uptake by macrophages or the reticuloendothelial system through opsonization are the main drawbacks of magnetic nanoparticles such as FOMNPs [34]. The advised approach to overcoming these drawbacks is crosslinking the coating molecules, especially with polymers, e.g., chitosan and dextran, while protecting these nanoparticles from opsonization by forming a hydrogel layer on their surface [34]. Therefore, in a future study, we will try to

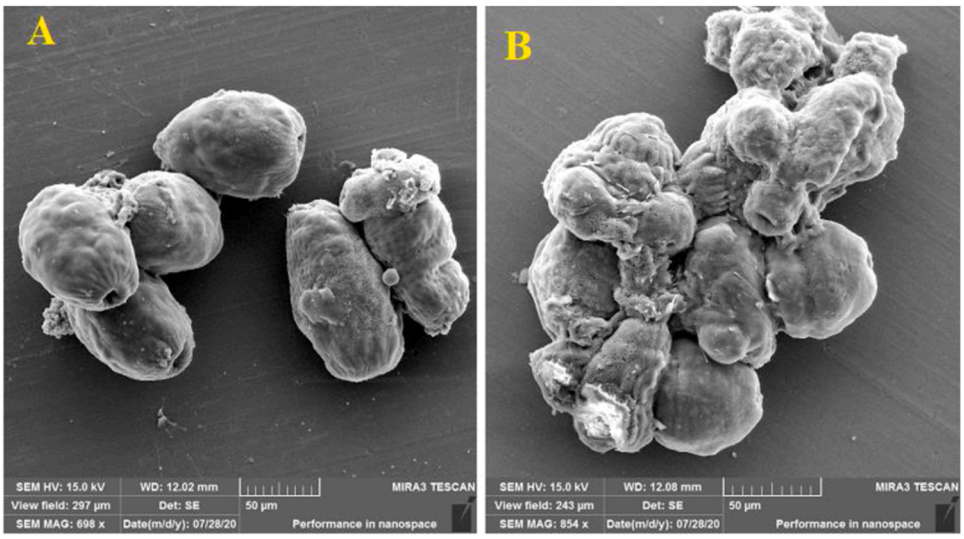

Fig. 5. Exterior ultra-structural effects of magnetic iron oxide nanoparticles covered by piroctone olamine on hydatid cyst protoscoleces by scanning electron microscopy. A: protoscoleces treated with normal saline and B: protoscoleces treated with the magnetic iron oxide nanoparticles.

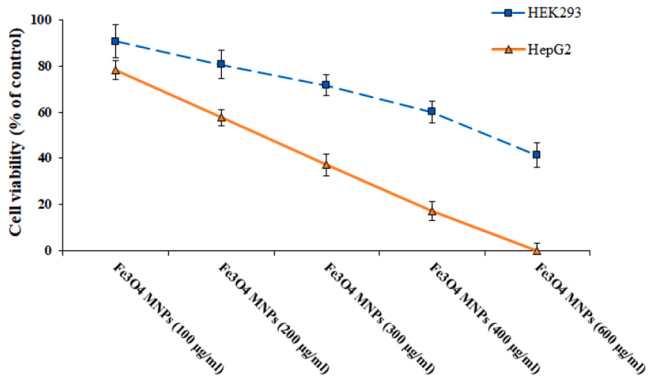

Fig. 6. Effect of different concentrations of magnetic iron oxide nanoparticles covered by piroctone olamine on viability of human normal embryonic kidney (HEK293) and human hepatocellular carcinoma (HepG2) cell. n = 3 (mean±sd).

Fig. 7. The liver and peritoneum hydatid cysts after treatment of the infected mice with different concentrations of magnetic iron oxide nanoparticles covered by piroctone olamine.

load these nanoparticles with polymers, e.g., chitosan and dextran.

4. Conclusion

The results of this experimental study revealed the potent in vitro protoscolicidal effects of FOMNPs covered with piroctone olamine against hydatid cyst protoscoleces through direct effects on the cell wall and indirect effects via apoptosis induction. Our results also indicated the promising effect in terms of controlling hydatid cysts in an animal model of these cysts. Although we reported that these nanoparticles are safe for human normal cells, more investigations are required to clarify their toxicity and precise mechanisms of action.

Table 1
In vivo effects of various doses of magnetic iron oxide nanoparticles coated with PO (FOMNPsP) on number, size and weight of hydatid cysts in mice of the tested groups.

Drug	Mean No. of cysts	Mean of size (mm)	Cyst weight (g)
Control (treated with normal saline)	13	4.36 ± 3.63	0.42 ± 0.31
FOMNPsP 20 mg/mL	9	3.78 ± 3.13	0.28 ± 0.196
FOMNPsP 40 mg/mL	7	2.23 ± 1.14	0.13 ± 0.078
Albendazole 200 mg/kg	6	1.96 ± 1.12	0.096 ± 0.046

Funding

Not applicable.

Ethical statement

This research was agreed by the Ethics Committee of the Lorestan University of Medical Sciences, Iran (IR.LUMS.REC.1401.246).

CRediT authorship contribution statement

Mojtaba Shakibaie: Study design and experiments. **Yosra Raziani:** Data collection, Critical revision of the manuscript. **Koroush Cheraghipour:** Data collection. **Javad Ghasemian Yadegari:** Interpretation and data analysis. **Hossein Mahmoudvand:** Supervisor, Writing the manuscript draft.

Conflict of interest statement

The authors declare that they have no known competing financial interests or personal relationships that could have appeared to influence the work reported in this paper.

Appendix A. Supplementary material

Supplementary data associated with this article can be found in the online version at doi:10.1016/j.biopha.2023.114536.

References

[1] P. Moro, P.M. Schantz, Echinococcosis: a review, Int. J. Infect. Dis., 13(2), 2009, pp. 125–33.

[2] J. Eckert, R.C. Thompson, historical aspects of echinococcosis, Adv Parasitol., 95, 2017, pp. 1–64. Epub 2016 Sep 29. PMID: 28131361 ⟨DOI: 10.1016/bs.apar.2016.07.003⟩.

[3] A. Siracusano, A. Teggi, E. Ortona, Human cystic echinococcosis: old problems and new perspectives, Interdiscip. Perspect. Infect. Dis. (2009). Jan 1;2009.

[4] N. Solomon, P.J. Fields, F. Tamarozzi, E. Brunetti, C.N.L. Macpherson, Expert reliability for the World Health Organization standardized ultrasound classification of cystic echinococcosis. Am. J. Trop. Med. Hyg., 96(3), 2017, pp. 686–691. Epub 2017 Apr 6. PMID: 28070008; PMCID: PMC5361546 ⟨DOI: 10.4269/ajtmh.16-0659⟩.

[5] N.I. Agudelo Higuita, E. Brunetti, C. McCloskey, Cystic echinococcosis, J. Clin. Microbiol., 54(3), 2016, pp. 518–23. Epub 2015 Dec 16. PMID: 26677245; PMCID: PMC4767951 ⟨DOI: 10.1128/JCM.02420-15⟩.

[6] M. Stojkovic, M. Zwahlen, A. Teggi, K. Vutova, C.M. Cretu, R. Virdone, P. Nicolaidou, N. Cobanoglu, T. Junghanss, Treatment response of cystic echinococcosis to benzimidazoles: a systematic review, PLoS Negl. Trop. Dis. 3 (9) (2009), e524. Sep 29.

[7] V. Velasco-Tirado, M. Alonso-Sardón, A. Lopez-Bernus, Á. Romero-Alegría, F. J. Burguillo, A. Muro, A. Carpio-Pérez, J.L. Bellido, J. Pardo-Lledias, M. Cordero, M. Belhassen-García, Medical treatment of cystic echinococcosis: systematic review and meta-analysis, BMC Infect. Dis. 18 (1) (2018) 1–9.

[8] T. Junghanss, A.M. da Silva, J. Horton, et al., Clinical management of cystic echinococcosis: state of the art, problems, and perspectives, Am. J. Trop. Med. Hyg. 79 (3) (2008) 301–311.

[9] M.A. Rajabi, Fatal reactions and methaemoglobinaemia after silver nitrate irrigation of hydatid cyst, Surg. Pract. 13 (2009) 2–7.

[10] H.K. Besim, K. Karayalcin, O. Hamamci, C. Güngör, A. Korkmaz, Scolicidal agents in hydatid cyst surgery, HPB Surg. 10 (6) (1998) 347–351.

[11] L. Mohammed, H.G. Gomaa, D. Ragab, J. Zhu, Magnetic nanoparticles for environmental and biomedical applications: A review, Particuology 30 (2017) 1–4.

[12] T. Vangijzegem, D. Stanicki, S. Laurent, Magnetic iron oxide nanoparticles for drug delivery: applications and characteristics, Expert Opin. Drug Deliv. 16 (1) (2019) 69–78.

[13] L.S. Arias, J.P. Pessan, A.P. Vieira, T.M. Lima, A.C. Delbem, D.R. Monteiro, Iron oxide nanoparticles for biomedical applications: A perspective on synthesis, drugs, antimicrobial activity, and toxicity, Antibiotics 7 (2) (2018) 46.

[14] M. Puviani, E. Campione, A.M. Offidani, R. De Grandi, L. Bianchi, I. Bobyr, M. Giannoni, A. Campanati, M. Bottagisio, A. Bidossi, De, E. Vecchi, Effects of a cream containing 5% hyaluronic acid mixed with a bacterial-wall-derived glycoprotein, glycyrretinic acid, piroctone olamine and climbazole on signs, symptoms and skin bacterial microbiota in subjects with seborrheic dermatitis of the face, Clin. Cosmet. Investig. Dermatol. (2019) 285–293.

[15] Y. Kim, P. Alpmann, S. Blaum-Feder, S. Kraemer, T. Endo, D. Lu, D. Carson, I. G. Schmidt-Wolf, Increased in vivo efficacy of lenalidomide by addition of piroctone olamine, In Vivo 25 (1) (2011) 99–103.

[16] A.E. Albalawi, A.D. Alanazi, P. Baharvand, M. Sepahvand, H. Mahmoudvand, High potency of organic and inorganic nanoparticles to treat cystic echinococcosis: an evidence-based review, Nanomaterials 10 (12) (2020) 2538.

[17] M.R. Khorramizadeh, Z. Esmail-Nazari, Z. Zarei-Ghaane, M. Shakibaie, K. Mollazadeh-Moghaddam, M. Iranshahi, A.R. Shahverdi, Umbelliprenin-coated Fe3O4 magnetite nanoparticles: antiproliferation evaluation on human Fibrosarcoma cell line (HT-1080), Mater. Sci. Eng. C 30 (7) (2010), 1038-42.

[18] M. Niazi, M. Saki, M. Sepahvand, S. Jahanbakhsh, M. Khatami, M. Beyranvand, In vitro and ex vivo scolicidal effects of Olea europaea L. to inactivate the protoscolecs during hydatid cyst surgery, Ann. Med. Surg. 42 (2019) 7–10.

[19] H. Mahmoudvand, M. Pakravanan, M.R. Aflatoonian, A.K. Khalaf, M. Niazi, S. R. Mirbadie, A. Tavakoli Kareshk, M. Khatami, Efficacy and safety of Curcuma longa essential oil to inactivate hydatid cyst protoscoleces, BMC Complement. Altern. Med. 19 (2019) 1–7.

[20] H. Mahmoudvand, R. Tavakoli Oliaei, S.R. Mirbadie, F. Kheirandish, A. Tavakoli Kareshk, B. Ezatpour, H. Mahmoudvand, Efficacy and safety of Bunium persicum (Boiss) to inactivate protoscoleces during hydatid cyst operations, Surg. Infect. 17 (6) (2016) 713–719.

[21] H. Mahmoudvand, M. Pakravanan, F. Kheirandish, S. Jahanbakhsh, M. Sepahvand, M. Niazi, A. Rouientan, M.R. Aflatoonian, Efficacy and safety Curcuma zadoaria L. to inactivate the hydatid cyst protoscoleces, Curr. Clin. Pharmacol. 15 (1) (2020) 64–71.

[22] F. Ezzatkhah, A.K. Khalaf, H. Mahmoudvand, Copper nanoparticles: biosynthesis, characterization, and protoscolicidal effects alone and combined with albendazole against hydatid cyst protoscoleces, Biomed. Pharmacother. 136 (2021), 111257.

[23] IBM How to Cite IBM SPSS Statistics or Earlier Versions of SPSS, 2014. ⟨http://www-01.ibm.com/support/docview.wss?uid=swg21476197⟩, (Accessed 31 August 2014).

[24] S. Aryamand, S. Khademvatan, K. Hazrati Tappeh, B. Heshmatian, A. Jelodar, In vitro and in vivo scolicidal activities of Holothuria leucospilota extract and CeO2 nanoparticles against hydatid cyst, Iran. J. Parasitol., 14(2), 2019, pp. 269–279. PMID: 31543915; PMCID: PMC6737367.

[25] Q. Gan, X. Lu, Y. Yuan, J. Qian, H. Zhou, X. Lu, J. Shi, C. Liu, A magnetic, reversible pH-responsive nanogated ensemble based on Fe3O4 nanoparticles-capped mesoporous silica, Biomaterials 32 (7) (2011) 1932–1942.

[26] Y. Wei, G. Yin, C. Ma, Z. Huang, X. Chen, X. Liao, Y. Yao, H. Yin, Synthesis and cellular compatibility of biomineralized Fe3O4 nanoparticles in tumor cells targeting peptides, Colloids Surf. B Biointerfaces 107 (2013) 180–188.

[27] S.V. Zaika, II Baranova, T.V. Martyniuk, Features of the introduction of the component piroctone olamine to the foam base, in: Proceedings of the 10th International Pharmaceutical Conference, Science and Practice 2019, Lithuanian University of Health Sciences, 2019, p. 111.

[28] M. Khatami, H. Alijani, I. Sharifi, F. Sharifi, S. Pourseyedi, S. Kharazi, M.A. Lima Nobre, M. Khatami, Leishmanicidal activity of biogenic Fe3O4 nanoparticles, Sci. Pharm. 85 (4) (2017) 36.

[29] R. Dorostkar, M. Ghalavand, A. Nazarizadeh, M. Tat, M.S. Hashemzadeh, Anthelmintic effects of zinc oxide and iron oxide nanoparticles against Toxocara vitulorum, Int. Nano Lett. 7 (2) (2017), 157-64.

[30] D. Kannan, N. Yadav, S. Ahmad, P. Namdev, S. Bhattacharjee, B. Lochab, S. Singh, Pre-clinical study of iron oxide nanoparticles fortified artesunate for efficient targeting of malarial parasite, eBioMedicine 45 (2019), 261-77.

[31] R. Capela, R. Moreira, F. Lopes, An overview of drug resistance in protozoal diseases. Int. J. Mol. Sci., 20(22), 2019, p. 5748. PMID: 31731801; PMCID: PMC6888673 ⟨DOI: 10.3390/ijms20225748⟩.

[32] A. Gupta, S. Mumtaz, C.H. Li, I. Hussain, V.M. Rotello, Combatting antibiotic-resistant bacteria using nanomaterials, Chem Soc Rev., 48(2), 2019, pp. 415–427. PMID: 30462112; PMCID: PMC6340759 ⟨DOI: 10.1039/c7cs00748e⟩.

[33] A. Raghunath, E. Perumal, Metal oxide nanoparticles as antimicrobial agents: a promise for the future, Int. J. Antimicrob. Agents 49 (2) (2017), 137-52.

[34] A. Raghunath, E. Perumal, Metal oxide nanoparticles as antimicrobial agents: a promise for the future, Int. J. Antimicrob. Agents 49 (2) (2017), 137-52.